Title

CROSSED THERMAL BEAM COLLISION MECHANICS: REACTIONS OF Ca, Sr, AND Ba WITH HI AND LIMITS ON D? FOR CaI, SrI, AND BaI

Author

Mims, Charles A.

Publication Date

1972-03-01

LBL-489
Preprint

CROSSED THERMAL BEAM COLLISION MECHANICS: REACTIONS OF Ca, Sr, AND Ba WITH HI AND LIMITS ON D_0^o FOR CaI, SrI, AND BaI

Charles A. Mims, Shen-Maw Lin, and Ronald R. Herm

March 1972

AEC Contract No. W-7405-eng-48

DISCLAIMER

CROSSED THERMAL BEAM COLLISION MECHANICS: REACTIONS OF Ca, Sr, AND Ba WITH HI AND LIMITS ON D_0^o FOR CaI, SrI, AND BaI

Charles A. Mims, Shen-Maw Lin, and Ronald R. Herm*

Inorganic Materials Research Division,
Lawrence Berkeley Laboratory and
Department of Chemistry, University of California
Berkeley, California 94720

ABSTRACT

Angular distributions of MI (M=Ca, Sr, or Ba) products scattered from crossed thermal beams of HI and M are reported and compared with derived expressions for the angular distributions of the velocities of the center-of-mass. These comparisons provide estimates of the reaction threshold relative kinetic energy, E^*, of 2-5, 1.5-3, and 0-1 kcal/mole for the Ca, Sr, and Ba+HI reactions respectively. Energy conservation and these measured E^* values establish rigorous lower bounds for D_0^o (MI) of 65(CaI), 67(SrI), and 69(BaI) kcal/mole.

---

*Alfred P. Sloan Foundation Fellow.

The K + HBr → KBr + H reaction was the first studied by the crossed molecular beam technique.[1] Reactions of A + HB → AB + H where the masses of both A and B greatly exceed that of the hydrogen atom are kinematically unique in that the nature of the transformation between the laboratory (LAB) and center-of-mass (CM) coordinate systems requires[2] that the AB product appear in the LAB system with a velocity close to that of the velocity of the center-of-mass of the collision partners, $\vec{C}$. This makes it extremely difficult to elucidate the reaction energy and angle recoil distributions from measurements of the AB flux in the LAB, although Bernstein and co-workers[3] did manage to do so for the K + HBr and K + DBr reactions in an elegant experiment employing a velocity selected K beam and velocity analysis of the KBr product. However, this kinematic restriction on these reactions

makes possible the determination of the dependence of the reaction cross section, Q, on relative kinetic collision energy, E, by means of an experiment in which the two reactant beams are crossed with thermal velocity distributions. Here one argues that the heavy AB product which is detected must essentially recoil (in the LAB) along $\vec{C}$ and proceeds to calculate the angular distribution of $\vec{C}$ for various assumed forms of Q(E). The requisite theory was developed in Ref. 2 for an experiment in which the LAB

flux of AB product is measured and was applied to the data reported in Ref. 1 for the K + HBr reaction. This resulted in an estimated threshold relative kinetic energy, E^*, of ∿2.5-3 kcal/mole, although the agreement of the experimental data with the theoretical curve was not very good. A much smaller value of E^* for this K + HBr reaction was obtained in a more recent[4] measurement of the KBr flux formed upon crossing a velocity selected K beam by a thermal HBr beam. A recent crossed thermal beam experiment of the type analyzed in Ref. 2 has reported[5] $E^* \sim$ 2-3 kcal/mole for the K + HCl → KCl + H reaction.

Although gaseous reactions of group IIA alkaline earth atoms have apparently not yet been studied by conventional kinetics techniques, a number of molecular beam laboratories[6-11], including our own, have recently initiated studies of reactions of these atoms. In the work reported here, analyses of measured product MI (M=Ca, Sr, or Ba) LAB angular distributions provide values of E^* for the M + HI → MI + H reactions as well as rigorous lower limits on D_0^o (MI).

EXPERIMENTAL PROCEDURE

The apparatus is described in detail in Ref. 12. Although less versatile and sensitive, it is similar to the universal detector molecular beam scattering apparatus described in Ref. 13. The alkaline earth atom beam is formed by thermal effusion through a knife-edge slit from a resistively heated stainless steel oven containing the metallic vapor at ∿0.1-0.5 Torr. The

HI, at a reservoir pressure of ∿1-1.5 Torr, emerges from a "crinkly foil" many-channel source (∿0.012 cm channel radius, ∿0.5 cm long, ∿90% calculated porosity), is chopped at ∿39 Hz, and intersects the atom beam at a 90° angle after a total flight path of ∿5 cm. This results in a small ($\lesssim$ 1%) attenuation of the atom beam. The detector, housed in a differentially-pumped UHV chamber and able to see the entire beam collision zone, may be rotated in the plane defined by the two intersecting beams. The scattered species are ionized by electron bombardment, mass analyzed in an RF quadrupole massfilter, and detected, via electron multiplier amplification, on a PAR HR-8 lock-in amplifier referenced (with negligible phase shift) to the HI beam chopping frequency.

CROSSED THERMAL BEAM COLLISION MECHANICS

Although theoretical expressions for the flux density angular distributions of velocities of the center-of-mass are given in Ref. 2, the corresponding expressions for the number density distributions are not available in the literature. The calculations of the number density distributions presented in this section are straight forward extensions of the methods and results presented in Ref. 2; accordingly, the nomenclature employed in Ref. 2 is retained here.

The thermal beams of masses M_1 and M_2 and most probable source speeds α_1 and α_2 are assumed to collide at an angle γ defining an intersection volume τ. The relative collision velocity, $\vec{V}$, relative collision energy, E, and center-of-mass velocity, $\vec{C}$, are defined in terms of the velocities of particles in beams 1

and 2, $\vec{v}_1$ and $\vec{v}_2$, by:

$$\vec{V} = \vec{v}_1 - \vec{v}_2, \tag{1a}$$

$$M\vec{C} = M_1\vec{v}_1 + M_2\vec{v}_2, \tag{1b}$$

and $$E = \mu V^2/2, \tag{1c}$$

where the mass factors are given by

$$M = M_1 + M_2 \tag{2a}$$

and $$\mu = M_1M_2/M. \tag{2b}$$

Figure 1 includes a transformation diagram for the special case of $\gamma = 90°$ illustrating the relations of $\vec{v}_1$, $\vec{v}_2$, $\vec{V}$, $\vec{C}$, and θ, the angle between $\vec{v}_1$ and $\vec{C}$.

The number of reactive events per second, N, is written in Ref. 2 in terms of the number densities of beams 1 and 2 at the collision zone, n_1 and n_2, as

$$N = n_1n_2\tau A \int_0^\infty \int_0^\infty Q(V)Vv_1^2v_2^2 \tag{3}$$

$$X\exp\left\{(-v_1^2/\alpha_1^2) + (-v_2^2/\alpha_2^2)\right\} dv_1dv_2$$

where $A = 16/(\pi\alpha_1^3\,\alpha_2^3)$. This may also be written as

$$N = \int_0^\gamma \int_0^\infty P(\theta,C)\,dCd\theta \tag{4}$$

where $P(\theta,C)dCd\theta$ is the number of reactive collisions per second with center-of-mass speed between C and C+dC and direction between θ and $\theta+d\theta$. Equating N in Eqs. (3) and (4) and employing results

derived from the transformation equations (Eq.(1)) in Ref. 2, $P(\theta,C)$ is readily evaluated to give

$$P(\theta,C) = \beta Q(MC/m)\ F(\theta)\ C^6 \exp[-M^2C^2/m^2\alpha^2], \tag{5}$$

$$F(\theta) = m^{-1}\ \sin^2(\gamma-\theta)\ \sin^2\theta/\sin^5\gamma$$

where $MC/m = V$ and $\beta = n_1 n_2 \tau A M^7/M_1^3 M_2^3$. Equation (5) is written in terms of the velocity independent, angle dependent "effective mass" m and "effective thermal source speed" α derived in Ref. 2 as:

$$m^{-2}\sin^2\gamma = \frac{\sin^2(\gamma-\theta)}{M_1^2} - \frac{2\cos\gamma\ \sin(\gamma-\theta)\sin\theta}{M_1 M_2} + \frac{\sin^2\theta}{M_2^2}; \tag{6}$$

$$\alpha^2 = \frac{\sin^2\gamma}{m^2}\left\{\frac{\sin^2(\gamma-\theta)}{M_1^2\,\alpha_1^2} + \frac{\sin^2\theta}{M_2^2\alpha_2^2}\right\}^{-1}. \tag{7}$$

Integration of $P(\theta,C)$ over C yields the flux angular distributions derived in Ref. 2. However, most molecular beam studies of non-alkali scattering will prdbably employ an electron bombardment ionization detector. This is a number density detector so that the appropriate centroid distribution function becomes

$$B(\theta,C) = \delta P(\theta,C)/C, \tag{8}$$

where δ is a constant characterizing the detector sensitivity. Molecular beam experimentalist may occasionally want to employ Eqs. (5) or (8) directly. Thus, assuming that Q(E) were known, comparison of Eq. (5) or (8) with measurements of LAB velocities of the AB product of the kinematically constrained A + HB reaction

would provide a check against systematic apparatus errors. Additionally, these equations indicate the distribution in origin of the CM coordinate system and might be useful in estimating the loss of resolution in CM cross sections which results from the LAB → CM transformation for the case of crossed thermal beam experiments.

The angular distribution of $\vec{C}$ appropriate to a number density detector may now be calculated by integrating $B(\theta,C)$ over C. In analogy with observations in Ref. 2, the resulting angular distribution is naturally expressed as

$$B(\theta) = (\delta\beta/2)(m/M)^6 \, F(\theta) \, G(\alpha^{-2}) \tag{9}$$

in terms of the La place transform[14]

$$G(\alpha^{-2}) = \int_0^\infty e^{-Z/\alpha^2} \, Z^2 Q(Z) dZ \tag{10}$$

where $Z = 2E/\mu$. Fortunately, this tranform is known[14] for the following two simple forms of Q(E):

$$Q_A(E) = Q_0 \, u(E-E^*); \tag{11a}$$

$$Q_B(E) = Q_0[1-(E^*/E)]u(E-E^*). \tag{11b}$$

Here, Q_0 and E^* are constants and u(t) is the unit step function, i.e.

$$u(t) = 0 \text{ for } t < 0, \; u(t) = 1 \text{ for } t > 0.$$

Model B is the well known[2] form of Q(E) which assumes a step function dependence on the component of $\vec{C}$ collision energy directed along the line-of-centers at impact. Figure 2 includes a comparison of Q(E) for Models A and B.

The $B(\theta)$ expressions obtained from Eqs. (9) and (10) for $Q(E)$ functions given by Eqs. (11a) and (11b) become:

$$B_A(\theta) = B_0(\theta)[2\alpha^6+2V^{*2}\alpha^4+V^{*4}\alpha^2] \tag{12a}$$

and $$B_B(\theta) = B_0(\theta)[2\alpha^6+V^{*2}\alpha^4] \tag{12b}$$

where $E^* = \mu V^{*2}/2$ and $B_0(\theta)$ is given by

$$B_0(\theta) = (\delta\beta Q_0/2)(m/M)^6 F(\theta)\exp(-V^{*2}/\alpha^2). \tag{13}$$

Note that $B_A(\theta)$ and $B_B(\theta)$ are identical in the limit that $E^*=0$. A detailed discussion of the dependences of $B_A(\theta)$ and $B_B(\theta)$ on V^* and γ is given in Ref. 12a.

EXPERIMENTAL RESULTS

Figures 1 and 2 show comparisons of the measured MI product angular distributions from the Ba, Sr, and Ca+HI reactions with angular distributions of $\vec{C}$ calculated from Eqs. (12) and (13). The LAB $\leftrightarrow$ CM transformation diagram for the Ba+HI reaction which is included in Fig. 1 indicates that the LAB BaI scattering velocity might deviate significantly in direction from that of $\vec{C}$. The maximum possible deviation may be estimated from the largest BaI CM recoil speed shown in this diagram, as we estimate the enthalpy of reaction as $\Delta H^\circ \gtrsim -10$ kcal/mole; the extent of deviations for the Sr and Ca reactions should resemble that for the Ba reaction. We have explicitly calculated MI LAB angular distributions for all three reactions for various assumed CM angular distributions and product recoil energies, E', by numerical

integrations of the CM → LAB transformations over thermal beam velocity distributions. These calculated MI LAB angular distributions were always broader than the angular distributions of $\vec{C}$ calculated for $E^*=0$, although the additional breadths were negligible unless $E' > \sim 5$ kcal/mole. Thus, the fact that the angular distributions of $\vec{C}$ calculated for $E^*=0$ are broader than the measured LAB SrI and CaI angular distributions shown in Figs. 1 and 2 clearly indicates finite values of E^* for these two reactions. Further support for the negligible deviation of the MI LAB recoil velocity from $\vec{C}$ which is assumed in this work is provided by the product KBr velocity analysis experiments reported in Ref. 3b. These experiments strongly suggested that most of the exoergicities of the K+HBr and DBr reactions appear as KBr internal excitation.

The quality of the fits of the measured BaI, SrI, and CaI angular distributions to angular distributions of $\vec{C}$ calculated from Eqs. (12) and (13) is clearly insufficient to permit any choice between reaction Models A and B. However, this insensitivity suggest that E^* estimates arrived at by fitting LAB MI angular distributions to calculated $B(\theta)$ functions should be relatively independent of the reaction model assumed. The quality of the fit for the Ba+HI reaction is rather good, better than that obtained in previous studies of the K+HBr[2] and HCl[5] reactions, whereas the fits to the Sr and Ca+HI data are less gratifying. In general, the peaks in the calculated $B(\theta)$ curves are seen to be shifted too far towards the alkaline

earth beam for E^* values which best fit the widths of the measured MI angular distributions. In view of the sharp angular beam profiles shown in Fig. 2, this discrepancy is most likely due to a non-thermal HI beam velocity distribution. The relatively small deviations from a thermal velocity distribution which have been reported[15] for a capillary beam source are not sufficient to account for the discrepancies observed here. However, Blais and Cross[16], employing a "crinkly foil" multi-channel source similar to that employed here, reported a velocity distribution for a Br_2 beam with a breadth characteristic of the source temperature, but with a most probable velocity considerably higher than that of the thermal distribution. We estimate that their reported deviation from the thermal distribution should provide an upper limit to the deviation of our HI velocity distribution because our HI flow rate was somewhat less than their reported Br_2 flow rate. We have numerically calculated angular distributions of $\vec{C}$ as a function of E^* for reaction Models A and B for the velocity distribution reported by Blais and Cross, scaled to reflect the mass difference between HI and Br_2. The widths of these numerically calculated distributions are practically the same as those of the corresponding thermal distributions, although the peaks are shifted towards the HI beam, in better agreement with the measured MI angular distributions.

Ranges of E^* values for the Ca, Sr, and Ba+HI reactions which are indicated by the data shown in Figs. 1 and 2 are given in Table I. These E^* ranges were arrived at by seeking the best fits

of the MI measured angular distributions to the calculated thermal angular distributions of $\vec{C}$; particular emphasis was placed on fitting the widths of the measured MI distributions. Additional support for the E^* values assigned here is provided by a comparison of the absolute MI^+ signals measured in this experiment with MX^+ signals measured, in the same apparatus, when studying reactions of M with Cl_2, Br_2, and ICl. This comparison suggest, for example, that E^* cannot much exceed 5 kcal/mole for the Ca+HI reaction if one assumes zero activation energy for the halogen molecule reactions.

No reactively scattered MX signals were observed from crossed beams of either Mg and HI or Ba and HF. If one assumes that the Q_0 constants in Eq. (11) for these reactions are comparable to those for Ca, Sr, and Ba+HI, this inability to observe reaction in the apparatus employed here would imply that $E^* > \sim 7$ kcal/mole for these two reactions. This might simply be a consequence of the Mg+HI reaction energetics, as D_0^o (MI) is not known well, but is likely[17,18] to be considerably less than D_0^o (HI). However, the behavior of the Ba+HF reaction cannot be rationalized in this manner, as the most recent value[19] for D_0^o (BaF) exceeds that of D_0^o (HF).

CaI, SrI, AND BaI BOND DISSOCIATION ENERGIES

As the techniques are applied to a wider variety of chemical reactions, studies of reaction dynamics may be expected to establish limits on a number of bond dissociation energies which are difficult to measure directly. For example, recent molecular

beam electronic chemiluminescence experiments[6] have established lower limits on D_0^o of BaO, BaCl, and SrCl. In the experiments reported here, a minimum of E^* relative kinetic energy is shown to be sufficient for the reactions of Ca, Sr, and Ba with HI. At the temperatures employed, the HI has negligible vibrational excitation and an average rotational energy given by RT_{HI}. The product recoil energy, E', and internal excitation, W', are related by energy conservation to the reactant energy by:

$$D_0^o\ (MI) = D_0^o\ (HI) - E^* - RT_{HI} + E' + W'. \qquad (14)$$

In his most recent compilation of bond energies of diatomic molecules, Gaydon[17] regards the experimental data on the bond energies of CaI, SrI, and BaI as unreliable and refers to ionic model calculations by Krasnov and Karaseva[18] for the best estimates. Since D_0^o (HI) is known[17] to be 70.6 kcal/mole, rigorous lower limits on D_0^o of CaI, SrI, and BaI may be calculated from Eq. (14) and upper limits for E^* given in Table I by assuming that E'+W' = 0. Table I shows a comparison of these lower limits with the ionic model estimates reported in Ref. 18.

ACKNOWLEDGEMENT

This work was supported by the U.S. Atomic Energy Commission through the Lawrence Berkeley Laboratory.

REFERENCES

1. E.H. Taylor and S. Datz, J. Chem. Phys. 23, 1711 (1955).
2. S. Datz, D.R. Herschbach, and E.H. Taylor, J. Chem. Phys. 35, 1549 (1961).
3. (a) A. E. Grosser, A.R. Blythe, and R.B. Bernstein, J. Chem. Phys. 42, 1268 (1965); (b) K.T. Gillen, C. Riley, and R.B. Bernstein, J. Chem. Phys. 50, 4019 (1969).
4. D. Beck, E.F. Greene, and J. Ross, J. Chem. Phys. 37, 2895 (1962).
5. T.J. Odiorne and P.R. Brooks, J. Chem. Phys. 51, 4676 (1969).
6. (a) Ch. Ottinger and R.N. Zare, Chem. Phys. Letters 5, 243 (1970); (b) C.D. Jonah and R.N. Zare, Chem. Phys. Letters 9, 65 (1971); (c) C.D. Jonah, R.N. Zare, and Ch. Ottinger, J. Chem. Phys. 56, 263 (1972).
7. C. Batalli-Cosmovici and K.W. Michel, Chem. Phys. Letters 11, 245 (1971).
8. J. Fricke, B. Kim, and W.L. Fite, Abstracts of Papers of the 7^{th} International Conference on the Physics of Electronic and Atomic Collisions (North Holland Publishing Company, Amsterdam, 1971), pp. 37-38.
9. F. Engelke, Universität Freiburg (private communication).
10. R.B. Bernstein, University of Wisconsin (private communication).
11. D.R. Herschbach, Harvard University (private communication).
12. (a) C.A. Mims, Ph.D. thesis, University of California, Berkeley, California, 1972; (b) S.-M. Lin, Ph.D. thesis, University of California, Berkeley, California, 1972.

13. Y.T. Lee, J.D. McDonald, P.R. LeBreton, and D.R. Herschbach, Rev. Sci. Instr. 40, 1402 (1969).

14. M. Abramowitz and I.A. Stegun (Eds.), Natl. Bur. Std. (US) Appl. Math. Ser. 55, 1020-1030 (1964).

15. D.R. Olander, R.H. Jones, and W.J. Siekhaus, J. App. Phys. 41, 4388 (1970); W.J. Siekhaus, R.H. Jones, and D.R. Olander, J. App. Phys. 41, 4392 (1970).

16. N.C. Blais and J.B. Cross, J. Chem. Phys. 52, 3580 (1970).

17. A.G. Gaydon, Dissociation Energies and Spectra of Diatomic Molecules (3rd Ed.) (Chapman and Hall Ltd., London, 1968).

18. K.S. Krasnov and N.V. Karaseva, Optics and Spectros. 19, 14 (1965).

19. D.L. Hildebrand, J. Chem. Phys. 48, 3657 (1968).

Table I. M+HI → H + MI reaction threshold energies and lower limits for D_0^o (MI).[a]

Group IIA atom, M	Measured threshold relative collision energy, E*	D_0^o(MI) estimates of Ref. 18	Lower limits for D_0^o(MI) provided by this work
Ca	2-5	75 ± 15	65
Sr	1.5-3	80 ± 15	67
Ba	0-1	85 ± 15	69

[a]All energies are given in kcal/mole.

FIGURE CAPTIONS

Fig. 1. The solid data points show measured LAB angular distributions of BaI and SrI products of the M+HI reactions. The solid curves give number density angular distributions of $\vec{C}$ calculated from Eqs. (12) and (13) for reaction Model B for different assumed values of E^*; the dashed curves show similar calculations for reaction Model A. The theoretical and measured distributions are normalized to the same peak intensity. Also shown is a LAB↔CM transformation diagram for the Ba+HI reaction. This is drawn for the $\gamma=90°$ intersection angle employed in this work and for Ba and HI velocities corresponding to the most probable collision event (calculated assuming thermal velocity distributions and an energy independent collision cross section). The diagram also shows the relative velocity $\vec{V}$ and center-of-mass velocity, $\vec{C}$. The circles are drawn for BaI CM recoil speeds corresponding to typical possible product recoil energies of 1, 2, 5, and 10 kcal/mole.

Fig. 2. Measured LAB angular distributions of CaI product of the Ca+HI reaction are plotted as solid data points in both the upper and lower panels; different data point symbols show results measured on different pumpdowns. Conventions for the solid and dashed calculated curves are the same as in Fig. 1. Also shown are (1) a diagram defining the LAB scattering angle, (2) angular profiles of the HI and

the alkaline earth beams, and (3) a comparison of the energy dependent cross sections in reaction Models A and B, calculated from Eqs. (11a) and (11b).

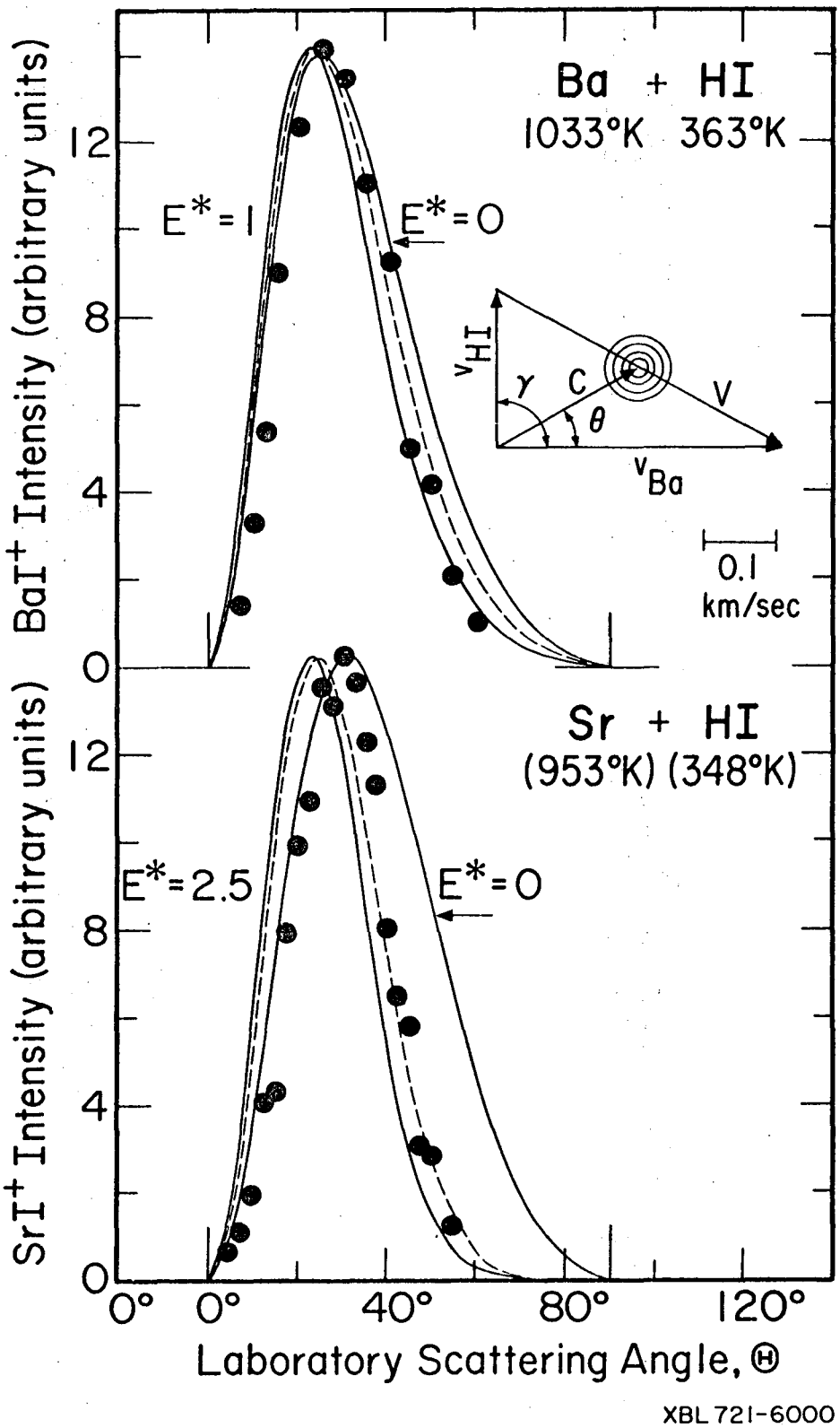
Ba + HI
1033°K 363°K
E*=1
E*=0
v_{HI}
γ
C
θ
V
v_{Ba}
0.1
km/sec
Sr + HI
(953°K) (348°K)
E*=2.5
E*=0
BaI+ Intensity (arbitrary units)
SrI+ Intensity (arbitrary units)
0
4
8
12
0°
0°
40°
80°
120°
Laboratory Scattering Angle, Θ
XBL 721-6000

Fig. 1.

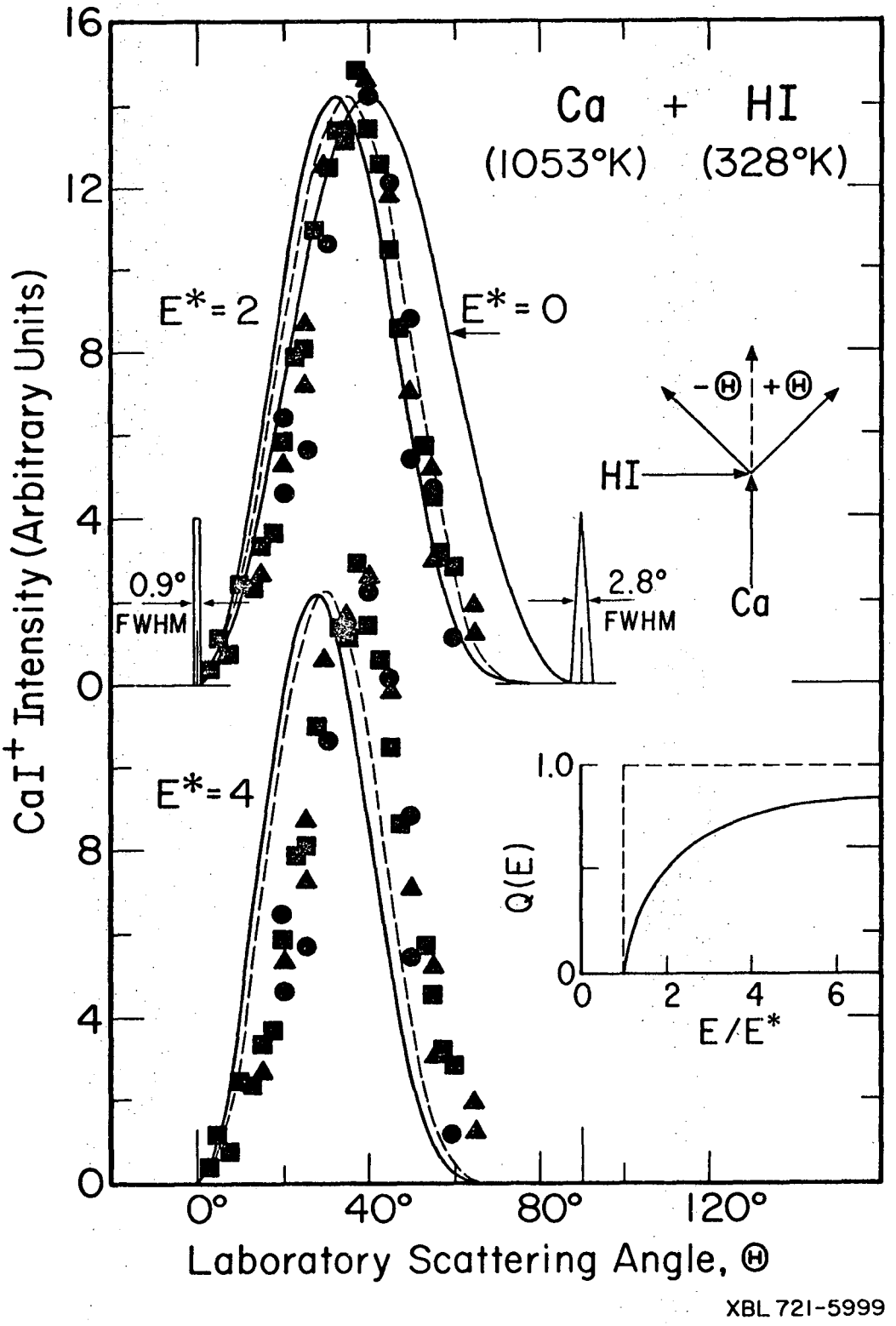
Ca + HI
(1053°K) (328°K)
E*=2
E*=0
E*=4
0.9° FWHM
2.8° FWHM
-Θ +Θ
HI
Ca
Q(E)
1.0
0
0 2 4 6
E/E*
CaI+ Intensity (Arbitrary Units)
16
12
8
4
0
8
4
0
0° 40° 80° 120°
Laboratory Scattering Angle, Θ
XBL 721-5999

Fig. 18.

TECHNICAL INFORMATION DIVISION
LAWRENCE BERKELEY LABORATORY
UNIVERSITY OF CALIFORNIA
BERKELEY, CALIFORNIA 94720